Stretchability of encapsulated electronics

J. Wu,[1] Z. J. Liu,[2] J. Song,[3] Y. Huang,[4,a)] K.-C. Hwang,[1] Y. W. Zhang,[2] and J. A. Rogers[5,a)]
[1]*AML, Department of Engineering Mechanics, Tsinghua University, Beijing 100084, China*
[2]*Institute of High Performance Computing, Singapore 138612*
[3]*Department of Mechanical and Aerospace Engineering, University of Miami, Coral Gables, Florida 33146, USA*
[4]*Departments of Civil/Environmental and Mechanical Engineering, Northwestern University, Evanston, Illinois 60208, USA*
[5]*Department of Materials Science and Engineering, University of Illinois, Urbana, Illinois 61801, USA*

(Received 5 July 2011; accepted 22 July 2011; published online 11 August 2011)

Stretchable and flexible electronics offer the performance of conventional wafer-based systems but can be stretched like a rubber band, twisted like a rope, and bent over a pencil. Such a technology offers new application opportunities, in areas of surgical and diagnostic implements that naturally integrate with the human body to provide advanced capabilities, to curvilinear devices such as hemispherical "eyeball" cameras. In practice, stretchable and flexible electronic systems require encapsulation layers to provide mechanical and environmental protection. This paper establishes a simple, analytical model for the optimal design of encapsulation. © *2011 American Institute of Physics*. [doi:10.1063/1.3624848]

Emerging research in the electronics seeks to develop stretchable and flexible technologies that offer the performance of conventional wafer-based devices, but with the ability to be stretched and compressed like a rubber band.[1,2] This type of technology offers many new application opportunities, ranging from bio-inspired design of cameras[3,4] to surgical and diagnostic implements that provide advanced therapeutic capabilities.[5–12]

In one approach, silicon islands, on which the active devices are fabricated, are printed on a pre-stretched elastometric [e.g., poly(dimethylsiloxane) (PDMS)] substrate to fabricate stretchable electronics. The interconnects between active devices are loosely bonded to the substrate such that releasing the pre-strain causes the interconnects to buckle out of the substrate surface and form arc-shaped structures, as illustrated in Fig. 1(a). The deformation localizes only to the interconnects after buckling and gives very small strains in the device islands. This leads to an overall stretchability of the combined system of the device islands and interconnects. The buckle amplitude A_0 is proportional to the interconnect length L_{bridge} and increases with the pre-strain ε_{pre} by $A_0 = (2L_{\text{bridge}}/\pi)\sqrt{\varepsilon_{\text{pre}}/(1+\varepsilon_{\text{pre}}) - \varepsilon_c}$,[13] where $\varepsilon_c = 4\pi^2\,\overline{EI_{bridge}}\,/(\overline{Eh}_{\text{bridge}}L_{\text{bridge}}^2)$ is the critical buckling strain and $\overline{EI}_{\text{bridge}}$ and $\overline{Eh}_{\text{bridge}}$ are the interconnect bending and tensile stiffness (per unit width), respectively. For an interconnect made of n layers of materials, the tensile stiffness is $\overline{Eh}_{\text{bridge}} = \sum_{i=1}^{n}\overline{E}_i h_i$, where $\overline{E}_i = E_i/(1-\nu_i^2)$ is the plane-strain modulus and h_i is the thickness of the ith layer from the top surface. The bending stiffness is $\overline{EI}_{\text{bridge}} = \sum_{i=1}^{n}\overline{E}_i h_i\{b - [\sum_{j=1}^{i} h_j - (h_i/2)]\}^2 + (\sum_{i=1}^{n}\overline{E}_i h_i^3/12)$, where b is the distance between the top surface and neutral mechanical plane and is given by $b = \sum_{i=1}^{n}\{\overline{E}_i h_i \times[\sum_{j=1}^{i} h_j - (h_i/2)]\}/\overline{Eh}_{\text{bridge}}$.

In practice, as illustrated in Fig. 1(b), an encapsulation layer of compliant elastomeric material is casted and cured on top of the buckled interconnects and device islands to provide mechanical and environmental protection and to minimize any restrictions on free motion of the buckled interconnects to avoid reductions in the stretchability.[14] This Letter establishes an analytic mechanics model for the optimal design of encapsulation layer for stretchable electronics. The model is validated by comparing with the finite element analysis and experiments.

The amplitude of buckled interconnect does not change when the encapsulation layer is casted and cured, but it changes to $A_0 + A$ after the encapsulated system is stretched, where A is the change of buckle amplitude due to the applied strain $\varepsilon_{\text{applied}}$. Each interconnect is modeled as a beam, which gives the

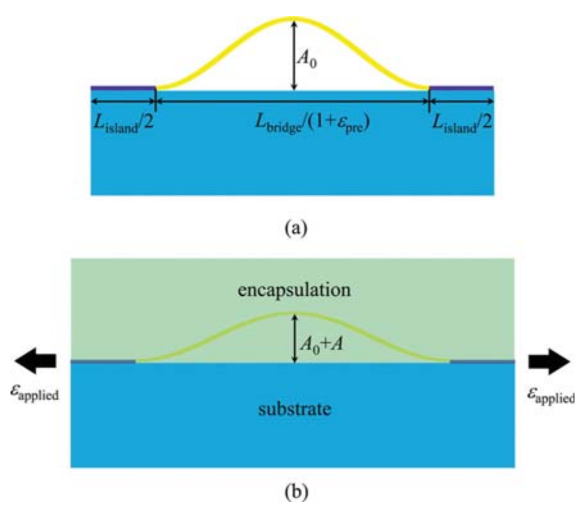

FIG. 1. (Color online) (a) A schematic diagram of noncoplanar mesh structure prior to encapsulation; (b) the encapsulated system subject to stretching.

a)Authors to whom correspondence should be addressed. Electronic addresses: y-huang@northwestern.edu and jrogers@illinois.edu.

bending energy $U_{\text{bending}} = (\pi^4 \overline{EI}_{\text{bridge}}/L_{\text{bridge}}^3)(A_0 + A)^2$.[13] The membrane strain in the interconnect is[13]

$$\varepsilon_{\text{membrane}} = \frac{\pi^2}{4L_{\text{bridge}}^2}(A_0 + A)^2 + \frac{\varepsilon_{\text{applied}} - \varepsilon_{\text{pre}}}{1 + \varepsilon_{\text{pre}}}, \qquad (1)$$

where the term $\pi^2(A_0 + A)^2/(4L_{\text{bridge}}^2)$ represents the contribution to the membrane strain from the finite rotation. Equation (1) gives the membrane energy in each interconnect $U_{\text{membrane}} = (\overline{Eh}_{\text{bridge}}/L_{\text{bridge}}/2)\varepsilon_{\text{membrane}}^2$. Without the encapsulation layer and applied strain, $A = 0$ and $\varepsilon_{applied} = 0$, the amplitude $A_0 = (2L_{\text{bridge}}/\pi)\sqrt{\varepsilon_{\text{pre}}/(1 + \varepsilon_{\text{pre}}) - \varepsilon_c}$ obtained from prior studies[13] gives the membrane strain $\varepsilon_{\text{membrane}} = -\varepsilon_c$.

The substrate and encapsulation layers are much thicker than the interconnects and device islands. Deformation of substrate and encapsulation layer is two-dimensional, being sinusoidal and exponential decay in the directions parallel and normal to the interconnects, respectively.[15] They are modeled as semi-infinite solids subject to the normal displacement on their surfaces $w = (A/2)[1 + \cos(2\pi X/L_{\text{bridge}})]$ for $|X| \le L_{\text{bridge}})/2$ due to buckling of the interconnects. For surfaces in contact with the device islands of size L_{island}, the normal displacement is $w = 0$ for $L_{\text{bridge}}/2 \le |X| \le (L_{\text{island}} + L_{\text{bridge}})/2$ since the device islands have negligible deformation as compared to the buckled interconnects. The normal displacement is periodic with the period $L_{\text{island}} + L_{\text{bridge}}$ and can be expressed as the Fourier series $w = A\left\{a_0/2 + \sum_{l=1}^{\infty} a_1 \cos[2l\pi X/(L_{\text{island}} + L_{\text{bridge}})]\right\}$, where the coefficients depend only on the interconnect line fraction $c = L_{\text{bridge}}/(L_{\text{island}} + L_{\text{bridge}})$ and are given by $a_l = [(1 - c^2 l^2) l\pi]^{-1} \sin(cl\pi)$ (which includes $a_0 = c$). The strain energy over each period for a semi-infinite solid subject to the above normal displacement is $(\pi/4)\overline{E}A^2 \sum_{l=1}^{\infty} l a_l^2$,[15] where $\overline{E}$ is the plane-strain modulus. The strain energy in the substrate and encapsulation layer (over the period $L_{\text{island}} + L_{\text{bridge}}$) is $U_{\text{substrate+encapsulation}} = (\pi/4)(\bar{E}_{\text{substrate}} + \bar{E}_{\text{encapsulation}})A^2 \Sigma_{l=1}^{\infty} l a_l^2$, where $\bar{E}_{\text{substrate}}$ and $\bar{E}_{\text{encapsulation}}$ are the plane-strain moduli of the substrate and encapsulation layers, respectively.

Minimization of total energy, $d(U_{\text{bending}} + U_{\text{membrane}} + U_{\text{substrate+encapsulation}})/dA = 0$, gives the following equation for the amplitude A:

$$\left(\frac{A_0 + A}{L_{\text{bridge}}}\right)^3 + \frac{4}{\pi^2}\left(\frac{\varepsilon_{\text{applied}} - \varepsilon_{\text{pre}}}{1 + \varepsilon_{\text{pre}}} + \varepsilon_c\right)\frac{A_0 + A}{L_{\text{bridge}}} + \frac{4(\bar{E}_{\text{substrate}} + \bar{E}_{\text{encapsulation}})}{\pi^5 \overline{Eh}_{\text{bridge}}} \times f\left(\frac{L_{\text{bridge}}}{L_{\text{island}} + L_{\text{bridge}}}\right)A = 0, \qquad (2)$$

where $f(c) = \sum_{l=1}^{\infty} l^{-1}(1 - c^2 l^2)^{-2} \sin^2(cl\pi)$ and $\overline{E}_{\text{encapsulation}}$ represents the effect of encapsulation layer against stretching. This cubic equation requires numerical method, but the stretchability of encapsulated system is obtained analytically, as shown in the following.

Near the limit of stretchability, the interconnects become rather flat such that the membrane strain is much larger than the bending strain and dominates in the interconnects. The stretchability is the maximum applied strain when $\varepsilon_{\text{membrane}}$ in Eq. (1) reaches the fracture strain ε_f (e.g., 1%) of the interconnects, which gives

$$A_0 + A = \frac{2L_{\text{bridge}}}{\pi}\sqrt{\frac{\varepsilon_{\text{pre}} - (\varepsilon_{\text{applied}})_{\max}}{1 + \varepsilon_{\text{pre}}} + \varepsilon_f}. \qquad (3)$$

Its substitution into Eq. (2) then gives analytically the stretchability

$$(\varepsilon_{\text{applied}})_{\max} = \left[1 - \left(1 + \frac{\varepsilon_f + \varepsilon_c}{\lambda}\right)^{-2}\right][\varepsilon_{\text{pre}} - (1 + \varepsilon_{\text{pre}})\varepsilon_c] + (1 + \varepsilon_{\text{pre}})(\varepsilon_f + \varepsilon_c). \qquad (4)$$

It increases with the pre-strain ε_{pre} (linearly) and fracture strain ε_f and critical buckling strain ε_c of the interconnects. It also depends on the elastic moduli of the substrate and encapsulation, length, tensile stiffness, and line fraction of the interconnects via a single combination λ given by

$$\lambda = \frac{(\overline{E}_{\text{substrate}} + \overline{E}_{\text{encapsulation}})L_{\text{bridge}}}{\pi^3 \overline{Eh}_{\text{bridge}}} f\left(\frac{L_{\text{bridge}}}{L_{\text{island}} + L_{\text{bridge}}}\right). \qquad (5)$$

The limit $\lambda = 0$ corresponds to no substrate and encapsulation layer and gives the stretchability $\varepsilon_{\text{pre}} + (1 + \varepsilon_{\text{pre}})\varepsilon_f$.

The maximum curvature near stretchability is $\kappa = \max(d^2w/dX^2) = (4\pi/L_{\text{bridge}})[1 + (\varepsilon_f + \varepsilon_c)/\lambda]^{-1} \times \sqrt{\varepsilon_{\text{pre}}/(1 + \varepsilon_{\text{pre}}) - \varepsilon_c}$. It can be verified that the bending strain $\sim\kappa h_{\text{bridge}}$ in the interconnects is much smaller than the membrane strain for the thin interconnects $h_{\text{bridge}} \ll L_{\text{bridge}}$.

Figure 2 shows the stretchability $(\varepsilon_{\text{applied}})_{\max}$ versus the non-dimensional parameter λ. The fracture strain of the interconnects is $\varepsilon_f = 1\%$, and pre-strain $\varepsilon_{\text{pre}} = 60\%$. A representative set of material properties and geometry parameters[14] includes

(1) Device islands: length of device island $L_{\text{island}} = 236\ \mu\text{m}$.

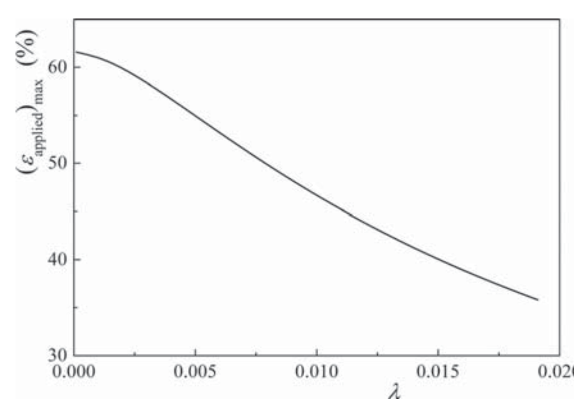

FIG. 2. The stretchability, $(\varepsilon_{\text{applied}})_{\max}$, versus the non-dimensional parameter λ for pre-strain $\varepsilon_{\text{pre}} = 60\%$.

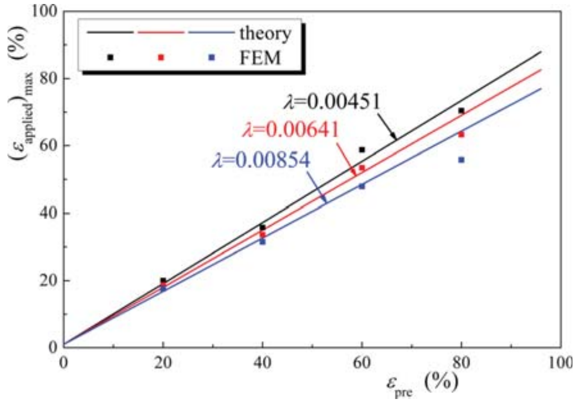

FIG. 3. (Color online) The stretchability, $(\varepsilon_{\text{applied}})_{\max}$, increases linearly with the pre-strain ε_{pre} for non-dimensional parameter $\lambda = 0.00451$, 0.00641, and 0.00854. Both analytical model and FEM are presented.

(2) Interconnects: made of polyimide ($h_1 = h_4 = 1.2$ μm, $E_1 = E_4 = 2.5$ GPa, $v_1 = v_4 = 0.34$), Au ($h_2 = 0.15\mu$m, $E_2 = 78$ GPa, $v_2 = 0.44$), and SiO_2 ($h_3 = 0.05$ μm, $E_3 = 70$ GPa, $v_3 = 0.17$), which give extremely small critical buckling strain $\varepsilon_c = 0.0032\%$ because of the long interconnects (length $L_{\text{bridge}} = 460\mu$m).

(3) Substrate: elastic modulus $E_{\text{substrate}} = 1.8$MPa, and Poisson's ratio $v_{\text{substrate}} = 0.48$.

(4) Encapsulation layer: elastic modulus ranging from $E_{\text{encapsulation}} = 0.1$MPa to 1.8 MPa, and Poisson's ratio $v_{\text{encapsulation}} = 0.48$.

These give the range of non-dimensional parameter $\lambda = 0.00451$ to 0.00854. The stretchabilities obtained from Eq. (4) for compliant ($E_{\text{encapsulation}} = 0.1$MPa) and relatively stiff (1.8 MPa) encapsulation layer are 55.8% and 48.9%, respectively, which agree well with the experimentally reported stretchability 55% and 49% (Ref. 14) and the finite element method simulation results 58.7% and 47.9%. The stretchability 55.8% for $E_{\text{encapsulation}} = 0.1$MPa is closer to the pre-strain 60% than that for $E_{\text{encapsulation}} = 1.8$MPa. Therefore the compliant encapsulation layer helps to retain the stretchability.

Figure 3 shows that the stretchability $(\varepsilon_{\text{applied}})_{\max}$ increases linearly with the pre-strain ε_{pre} for non-dimensional parameters $\lambda = 0.00451$, 0.00641, and 0.00854. The finite element method (FEM) is used to calculate the stretchability by equating the maximum strain in the interconnects obtained by FEM to the fracture strain ε_f. The 8-node, hexahedral brick element C3D8R in the FEM software ABAQUS (Ref. 16) is used for the substrate and encapsulation, and 4-node, multi-layer shell element S4R is used for the interconnects. These two types of elements are bonded by embedded element at the interface. The mesh is refined to ensure the convergence of numerical results. As shown in Fig. 3, the numerical results agree very well with the analytical solution in Eq. (4) for stretchability.

In summary, a simple, analytical expression is obtained for the stretchablility of mesh-type electronics on an elastomeric substrate, when encapsulated by a compliant elastomeric material. The stretchability increases with the pre-strain and the fracture strain of the interconnects. All other material and geometry parameters of the device islands, interconnects, substrate and encapsulation layer influence the stretchability via a single non-dimensional parameter λ. The simple, analytical expression for stretchability provides easily interpretable guidelines for the design of encapsulated stretchable electronics.

J.W. and Z.J.L. contribute equally to this work. Y.H. and J.A.R. acknowledge the supports from the NSF (Grant Nos. CMMI-0845294, ECCS-0824129, and OISE-1043143). Y.H. and K.C.H. acknowledge the supports from the NSFC and Ministry of Education of China. J.S. acknowledges the support from the NSF (Grant No. OISE1043161).

[1] S. R. Forrest, Nature **428**, 911 (2004).
[2] J. A. Rogers, T. Someya, and Y. Huang, Science **327**, 1603 (2010).
[3] H. C. Ko, M. P. Stoykovich, J. Song, V. Malyarchuk, W. M. Choi, C.-J. Yu, J. B. Geddes III, J. Xiao, S. Wang, Y. Huang, and J. A. Rogers, Nature **454**, 748 (2008).
[4] G. Shin, I. Jung, V. Malyarchuk, J. Song, S. Wang, H. C. Ko, Y. Huang, J. S. Ha, and J. A. Rogers, Small **6**, 851 (2010).
[5] T. Someya, T. Sekitani, S. Iba, Y. Kato, H. Kawaguchi, T. Sakurai, Proc. Natl. Acad. Sci. USA **101**, 9966 (2004).
[6] D.-H. Kim, J. Viventi, J. J. Amsden, J. L. Xiao, L. Vigeland, Y.-S. Kim, J. A. Blanco, D. Contreras, D. L. Kaplan, F. G. Omenetto, Y. Huang, K. C. Hwang, M. R. Zakin, B. Litt, and J. A. Rogers, Nat. Mater. **9**, 511 (2010).
[7] J. Viventi, D.-H. Kim, J. D. Moss, Y.-S. Kim, N. Annetta, D. J. Callans, J. Xiao, Y. Huang, J. A. Rogers, and B. Litt, Sci. Trans. Med. **2**, 24ra22(2010).
[8] S. Wagner, S. P. Lacour, J. Jones, P. I. Hsu, J. C. Sturm, T. Li, Z. Suo, Physica E **25**, 326 (2005).
[9] T. Stieglitz, Sens. Actuators, A **90**, 203 (2001).
[10] J.-U. Meyer, T. Stieglitz, O. Scholz, W. Haberer, and H. Beutel, IEEE Trans. Adv. Pack. **24**, 366 (2001).
[11] D.-H. Kim, N. Lu, R. Ghaffari, Y.-S. Kim, S. P. Lee, L. Xu, J. Wu, R.-H. Kim, J. Song, Z. Liu, J. Viventi, B. de Graff, B. Elolampi, M. Mansour, M. J. Slepian, S. Hwang, J. D. Moss, S.-M. Won, Y. Huang, B. Litt, and J. A. Rogers, Nat. Mater. **10**, 316 (2011).
[12] R.-H. Kim, D.-H. Kim, J. Xiao, B. H. Kim, S.-I. Park, B. Panilaitis, R. Ghaffari, J. Yao, M. Li, Z. Liu, V. Malyarchuk, D. G. Kim, A.-P. Le, R. G. Nuzzo, D. L. Kaplan, F. G. Omenetto, Y. Huang, Z. Kang, and J. A. Rogers, Nat. Mater. **9**, 929 (2010).
[13] J. Song, Y. Huang, J. Xiao, S. Wang, K. C. Hwang, H. C. Ko, D. H. Kim, M. P. Stoykovich, and J. A. Rogers, J. Appl. Phys. **105**, 123516 (2009).
[14] D.-H. Kim, Z. Liu, Y.-S. Kim, J. Wu, J. Song, H.-S. Kim, Y. Huang, K. C. Hwang, Y. Zhang, and J. A. Rogers, Small **5**, 2841 (2009).
[15] H. Jiang, Y. Sun, J. A. Rogers, and Y. Huang, Int. J. Solids Struct. **45**, 2014 (2008).
[16] *ABAQUS Analysis User's Manual V6.10* (Dassault Systèmes, Pawtucket, RI, 2010).